



Single and binary component adsorption of endocrine disrupting chemicals from aqueous solutions using calcium alginate/apricot stone-activated carbon composite beads

Nassima Djebri^a, Kamel Noufel^b, Nadia Boukhalfa^c, Dounia Sid^c, Mokhtar Boutahala^{c,*}

^aLaboratoire Matériaux et systèmes Electroniques (LMSE), Faculté des Sciences et de la Technologie, Faculté des Sciences de Bordj Bou Arreridj, El Annasser, 34000 BBA, Algérie

^bLaboratoire des Matériaux Inorganique (LMI), Faculté des Sciences, Université de Mohamed Boudiaf 28000, M'Sila, Algérie

^cLaboratoire de Génie des Procédés Chimiques (LGPC), Faculté de Technologie, Université Ferhat Abbas Sétif-1-19000, Sétif, Algérie, email: mboutahala@yahoo.fr (M. Boutahala)

Received 3 June 2019; Accepted 25 March 2020

ABSTRACT

Alginate gel (A) and activated carbon prepared from apricot stone (AC) were combined to prepare activated carbon alginate beads (A-AC) adsorbent and used to remove bisphenol A (BPA) and 2,4,5-trichlorophenol (TCP) from solution in single and binary system. The zero point charge determination (pHpzc), the scanning electron microscopy (SEM) and Fourier transform infrared spectroscopy (FTIR) analysis were carried out. The effects of pH solution (2–11), temperature (15°C, 25°C, 35°C, and 45°C), initial concentration (15–400 mg/L) and contact time were investigated. The adsorption processes fitted well with the pseudo-second-order kinetic model and Langmuir isotherm. Results showed that the maximum adsorption capacities of A-AC for the adsorption of BPA and TCP in single system are 419.3 and 444.3 mg/g at 25°C, respectively. In the binary system, a decrease was observed at the adsorbed amount to 291.2 mg/g for BPA and 430.2 mg/g for TCP. The thermodynamic parameters confirmed that the adsorption reaction was spontaneous and endothermic in nature. Desorption tests showed that the removal efficiency of A-AC for BPA and TCP decreased slightly after six regeneration cycles and were maintained at 83.2% and 77.6%, respectively. The results suggest that the use of A-AC beads is a feasible strategy for the removal of BPA and TCP.

Keywords: Adsorption; Apricot stone; Alginate; Composite; Competition; Emerging pollutant.

1. Introduction

Endocrine-disrupting compounds (EDCs) are an important class of emerging contaminants that have been detected in aquatic environments such as wastewater, groundwater, and surface water [1]. It is widely accepted that EDCs are highly dangerous to human beings, even at low concentration levels. They cause diseases and various disorders into the human body. In this context, the EDCs such as bisphenol (BPA), chlorophenol (CP), and their derivatives such as

trichlorophenol (TCP) are classified as toxic and carcinogenic pollutants and thereby pose serious hazards to aquatic living organisms [2,3]. Therefore, the removal of these pollutants is highly desirable and of considerable interests.

Various methods such as nanofiltration [4], reverse osmosis [5], advanced oxidation processes [6], ozone [7], and adsorption [8–12] have been utilized for the treatment of BPA and TCP polluted solutions. Adsorption has been proved as a cheap and highly effective method in the removal of pollutants from water [3,8]. Several adsorbents

* Corresponding author.

such as commercial activated carbons (AC) were used for the removal of different types of emerging pollutants [1,13], but their use is limited due to their high costs. This makes many researchers trying to prepare low cost alternative adsorbents, which may replace activated carbons used in pollution control through the adsorption process.

Recently, natural residue materials available in large quantities from nature have been used as low cost adsorbents [14]. Moreover, the use of these materials directly or after some treatments is becoming a vital concern because they represent unused resources, which causes disposal problems. The raw agricultural wastes such as agave bagasse, almond shell, coconut husks, barley straw, fruit peels, coffee grounds, olive stone, orange peel, etc., have been used as adsorbents for purification and removal of toxic pollutants [1].

Sodium alginate (A), a linear biopolymer has received more attention as an adsorbent for the removal of heavy metals. It was preferred over other materials because of its biodegradability, hydrophilicity, and abundance in nature. Moreover, the presence of carboxylate groups (COOH) in alginate provides the ability to form complexes with a variety of multivalent ions. However, alginate was modified into several forms to improve its adsorption capacity and mechanical strength. For instance, the alginate was blended with chitosan, humic acid, polyurethane, cellulose, carbon nanotubes, and clays to enhance the adsorption capacity for the removal of pollutants from aqueous solution [15–17].

It is known that the materials used in the adsorption processes lose their mass when they are used in a powder form after unit operations, which generates a huge waste and creates another problem for the environment [3]. Likewise, these powdered materials cannot be used in a fixed bed reactor because of the regeneration cost and clogging of the reactors [18]. In general, the encapsulation of adsorbent into alginate beads is an elegant solution to overcome this problem. Few studies have been devoted to adsorption on materials containing alginate and further research is needed in this area [8,15]. In this context, the purpose of this study is to prepare an appropriate adsorbent material by encapsulating the activated carbon in alginate beads to combine the properties and advantages of each of the two of them.

In the present work, activated carbon (AC) prepared from a modified apricot stone, alginate (A), and their composite (A-AC) were characterized by scanning electron microscopy

(SEM), Fourier transform infrared spectroscopy (FTIR), and zero point charge (pH_{PZC}). The BPA and TCP were selected as model of phenolic pollutants to examine the performance of A-AC composite. The A-AC adsorbent was investigated in single and binary systems in batch mode experiments. In order to determine the reusability of the A-AC loaded by BPA and TCP ions, six cycles of adsorption/desorption were carried out. To the best of our knowledge, there are very limited published informations on the adsorption of BPA/TCP in single and binary systems and few regeneration studies for the activated carbon obtained by apricot stone/alginate composite.

2. Materials and methods

2.1. Materials

Apricot stones were obtained locally (region of Setif-Algeria). Alginate (A), bisphenol A (BPA), 2,4,5-TCP, sodium chloride (NaCl), calcium chloride (CaCl_2), phosphoric acid (H_3PO_4) were all purchased from Sigma-Aldrich (USA). The physicochemical properties of phenolic compounds are given in Table 1. Distilled water were used in all experiments.

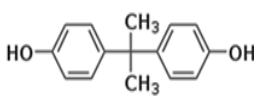
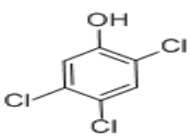
2.2. Preparation of activated carbon

The activated carbon was prepared by chemical activation using phosphoric acid according to the method of Shao et al. [19]. Briefly, chemical impregnation was carried out in a round-bottom flask reactor, where 20 g of precursor (Apricot Stone) reacted with a 40 wt.% H_3PO_4 solution at a ratio of 1:2 (AS/ H_3PO_4) under stirring for 6 h. After impregnation, the mixture was filtered under vacuum to remove the excess of phosphoric acid, and then the solid was calcined at 450°C for 1 h, defining a heating ramp of 10°C/min. The resulting carbon was washed with distilled water in order to remove the remaining phosphoric acid until the solution pH reaches 6.5. Finally, the solid was dried in an oven at 110°C for 24 h. The resulting material was named as activated carbon (AC).

2.3. Preparation of calcium alginate beads

For the preparation of (A) beads, 1% sodium alginate solution was added drop wise to 4% calcium chloride

Table 1
Physicochemical properties of the selected endocrine-disrupting compounds (EDCs)

Compound	MW (g/mol)	Water solubility (mg/L), at 25°C	Dissociation constant (pKa)	Log K_{ow}	Chemical structure
BPA ($\text{C}_{15}\text{H}_{16}\text{O}_2$)	228.29	120–300	9.6–10.2	3.32	
TCP ($\text{C}_6\text{H}_3\text{Cl}_3\text{O}$)	197.45	1,200	6.7–6.94	3.66	

solution. The water-soluble sodium alginate was converted to water-insoluble calcium alginate beads. All beads were then washed with deionized water several times to remove the excess of unbounded calcium chloride from beads surfaces. The washed beads were then dried and stored in a clean dry glass bottle. The resulting material was named as alginate beads (A).

2.4. Preparation of A-AC composite material

A solution of 1% sodium alginate was prepared in deionized water in a 250 mL flask under stirring for 2 h. The amount (2 g) of activated carbon (AC) was added. The mixture was stirred for 24 h at room temperature (25°C). The homogenous mixture was dropped into a flask containing CaCl₂ (4%, w/v) solution to produce calcium alginate/activated carbon (A-AC) composite beads. The collected beads were washed, dried, and stored in a clean dry glass bottles for subsequent use.

2.5. Characterization of adsorbents

The morphological structure of the investigated samples was examined by SEM using SEM model (JSM-6380-LV, JEOL, Tokyo, Japan).

FTIR analysis of the adsorbent before and after adsorption was carried out in KBr pellets in the range of 4,000–400 cm⁻¹ with 4 cm⁻¹ resolution using the Perkin-Elmer spectrum FTIR model 65 spectrometer.

The pH_{PZC} values of samples were obtained using the same method described by Djebri et al. [3]. In brief, the initial pHs (pH_i) of 0.01 M NaCl solutions (50 mL) were adjusted to a pH range of 2–12 using HCl or NaOH. Then, 0.2 g of adsorbent was added to each sample. The dispersions were stirred for 48 h at 25°C, and the final pH_f of the solutions were determined. The point of zero charge was obtained from a plot of (pH_f – pH_i) vs. pH_i.

2.6. Batch adsorption studies

The effect of solution pH on the adsorption onto A-AC was examined from pH 2 to 10. The adsorbate initial concentration (100 mg/L) with a solid dose (1 g/L) was kept constant. The adsorption experiments were conducted at a constant temperature of 25°C. The pH was adjusted using 0.1 and 1.0 M HCl or NaOH.

Time dependence adsorption of BPA and TCP was carried out from 0 to 96 h using 0.2 g of adsorbent with 200 mL of adsorbate solution at a constant temperature (25°C) with a concentration from 30 to 300 mg/L for BPA and from 15 to 400 mg/L for TCP. The concentration of adsorbate after recorded time intervals was determined. The adsorption capacity q_t (mg/L) at different contact time t (h) was determined using the following equation:

$$q_t = \frac{(C_0 - C_t) \cdot V}{m} \quad (1)$$

where C_t and C_0 (mg/L) are the concentrations of BPA or TCP at time t (h) and initial time, respectively, in the solution.

V is the volume of the solution (L) and m is the weight (g) of the adsorbent.

The adsorption of BPA and TCP was conducted in a static batch experiment. An aqueous solution of a certain concentration of adsorbate (10–500 mg/L) was shaken in bottles of 200 mL capacity with 1 g/L of adsorbent A-AC for 96 h. The supernatant liquid was separated out, where the equilibrium concentration of the BPA and TCP was determined using UV/Vis 1700 spectrophotometer at 276 and 290 nm, respectively.

Effect of temperature was examined at 15°C, 25°C, 35°C, and 45°C for 96 h. In these experiments, 0.2 g of adsorbent with 200 mL of 100 mg/L of BPA or TCP was employed. After shaking, the adsorption rate was measured. The adsorbed amount at equilibrium, q_e (mg/L) was calculated by:

$$q_e = \frac{(C_0 - C_e) \cdot V}{m} \quad (2)$$

The percentage removal (R %) by the adsorbent was expressed by:

$$R(\%) = \frac{(C_0 - C_e) \cdot 100}{C_0} \quad (3)$$

where C_e (mg/L) is the liquid – phase concentration of BPA or TCP at equilibrium.

2.7. Binary adsorption studies

The first step was to examine the adsorption of BPA at equilibrium (concentration of BPA ranging from 20 to 300 mg/L) in the presence of TCP (50 mg/L). For the next step, a series of binary solutions where the concentration of BPA was fixed at 50 mg/L, and the concentration of TCP were varied from 20 to 400 mg/L. These binary solutions were stirred at 200 rpm for 96 h at 25°C ± 1°C. A correction was applied for the spectrophotometric determination of residual concentrations in mixture systems using Eqs. (4) and (5):

$$C_{\text{BPA}} = \frac{k_{\text{TCP}2}d_{\lambda 1} - k_{\text{TCP}1}d_{\lambda 2}}{k_{\text{BPA}1}k_{\text{TCP}2} - k_{\text{BPA}2}k_{\text{TCP}1}} \quad (4)$$

$$C_{\text{TCP}} = \frac{k_{\text{BPA}1}d_{\lambda 2} - k_{\text{BPA}2}d_{\lambda 1}}{k_{\text{BPA}1}k_{\text{TCP}2} - k_{\text{BPA}2}k_{\text{TCP}1}} \quad (5)$$

where C_{BPA} , C_{TCP} , $k_{\text{TCP}1}$, $k_{\text{TCP}2}$, $k_{\text{BPA}1}$, $k_{\text{BPA}2}$, $d_{\lambda 1}$, and $d_{\lambda 2}$ are the concentrations of BPA and TCP, the calibration constants for BPA and TCP at their characteristic adsorption wavelength (i.e., k_1 and k_2), and the optical densities at the two wavelengths λ_1 and λ_2 , respectively.

2.8. Desorption and regeneration of adsorbent

Desorption study was conducted using ethanol as a desorption eluent. Adsorption was first conducted using the same procedure in section 2.6 (Batch adsorption studies). Then the A-AC with adsorbed BPA or TCP was separated

from the solutions. Subsequently, the supernatant solutions were discarded and the A-AC adsorbent was washed with distilled water. Finally, the BPA or TCP were desorbed from the A-AC with 50 mL of ethanol. To investigate the regeneration of the adsorbent, A-AC was reused after desorption in adsorption experiments and the process was repeated six times. The percentage of desorption of BPA or TCP was calculated from the following equation:

$$R\% = \frac{m_{\text{des}}}{m_{\text{ads}}} \times 100 \quad (6)$$

where m_{des} (mg) and m_{ads} (mg) are the amounts of desorbed and adsorbed BPA or TCP, respectively.

2.9. Error analysis

In order to test the best correlation of the experimental data, the regression R^2 and residual root-mean squared error (RMSE) using ORIGIN program (version 8) were evaluated using Eqs. (7) and (8). In addition, the Akaike information criterion (AIC) was determined by ORIGIN program (version 2018) using Eqs. (9) and (10).

$$R^2 = 1 - \frac{\sum_{n=1}^n (q_{e,t,\text{exp},n} - q_{e,t,\text{cal},n})^2}{\sum_{n=1}^n (q_{e,t,\text{exp},n} - q_{e,t,\text{exp},n})^2} \quad (7)$$

$$\text{RMSE} = \sqrt{\frac{1}{n} \sum_{i=1}^n (q_{e,t,\text{exp},n} - q_{e,t,\text{cal},n})^2} \quad (8)$$

$$\text{AIC} = 2p - 2\text{Ln}(L) \quad (9)$$

$$\text{Ln}(L) = 0.5 \times \left\{ -N \times \left(\text{Ln} 2\pi + 1 - \text{Ln} N + \sum_{i=1}^n x_i^2 \right) \right\} \quad (10)$$

where $q_{e,t,\text{exp}}$ and $q_{e,t,\text{cal}}$ are the experimental adsorption capacity at equilibrium ($q_{e,\text{exp}}$) or at any time ($q_{t,\text{exp}}$) and the calculated adsorption capacity at equilibrium $q_{e,\text{cal}}$ or at any time $q_{t,\text{cal}}$ from the models, respectively. N is the number of observations and p is the number of parameters. n is the sample size. $\text{Ln}(L)$ is the maximum log-likelihood of the estimated model. x_i are the residuals from the nonlinear least-squares fit.

3. Results and discussion

3.1. Characterization of A-AC composite adsorbent

FTIR spectra of A-AC before and after adsorption of BPA and TCP are depicted in Fig. 1. The broad absorption band at 3,300–3,600 cm^{-1} with a maximum at about 3,424 cm^{-1} is characteristic of the stretching vibration of hydrogen-bonded hydroxyl groups (from carboxyls, phenols, or alcohols) and adsorbed water onto A-AC [20]. The ν (C–H) stretching bands are detectable at 2,922 and 2,855 cm^{-1} . The strong asymmetric and weak symmetric stretching vibration bands of $-\text{COO}$ observed at 1,615 and 1,415 cm^{-1} are

caused by the alginate molecules [8,17]. The band at 800 cm^{-1} is attributed to out-of-plane deformation mode of C–H for different substituted benzene rings. After the adsorption of BPA and TCP onto A-AC, many functional groups shifted to different bands. The bands at 3,424; 1,615; 1,080; and 800 cm^{-1} transferred to higher frequencies at 3,481; 1,635; 1,111; and 811 for TCP and 3,441; 1,633; 1,097; and 811 for BPA, respectively. Whereas the peak at 1,415 cm^{-1} shifted slightly to a lower frequency band at 1,409 and 1,413 cm^{-1} , for BPA and TCP, respectively. On the contrary, the peaks at 630 and 476 cm^{-1} appeared after adsorption. These changes indicated the possible interaction of surface sites of A-AC with BPA and TCP [3].

SEM images were taken at 50 \times (Fig. 2a), 150 \times (Fig. 2b), and 25 \times (Fig. 2c) magnifications as shown in Fig. 2. The surface of activated carbon AC (Fig. 2b) is characterized by grooves, irregular ridges, channels, and bright spots, which appeared undulated due to the presence of intermittently spaced protrusions. The distribution of pore sizes is irregular with variable hole sizes, which implied a wide surface area for active sites for adsorption. The alginate beads A (Fig. 2a) have a smooth surface with streaks. The structure is homogeneous with a regular surface porosity and a relatively uniform morphology. In the case of A-AC beads (Fig. 2c), sphericity is confirmed, their surface is relatively smooth and has undulations. These beads exhibit a bright and clear morphology with a heterogeneous surface [21].

For better understanding of adsorption mechanism, the pH_{PZC} of A and AC (figure not shown) were determined and found to be 6.6 and 3.0, respectively; while the pH_{PZC} of A-AC was found to be 4.5 (see Fig. 3, Inset), indicating the acid character of A-AC surface, which is in agreement with the presence of acid groups appeared in the FTIR spectrum. Below the pH_{PZC} value, the surface of A-AC is positively charged, favoring the adsorption of anions via electrostatic forces attractions. Above the pH_{PZC} the surface has a negative charge, which favors the adsorption of cation species.

3.2. Effect of pH

The removal percentage of BPA and TCP by A-AC at different pH values is plotted in Fig. 3. As can be seen

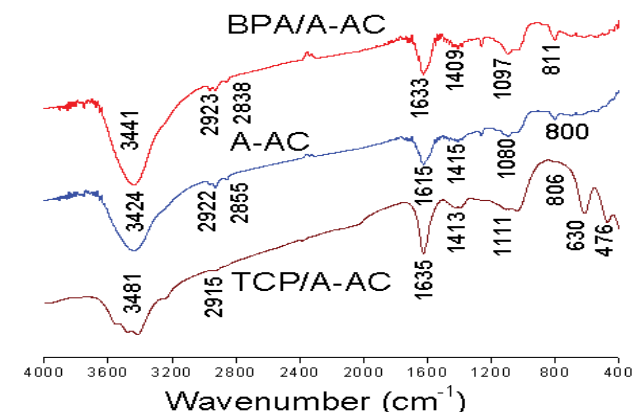


Fig. 1. FTIR patterns of A-AC before and after adsorption of BPA and TCP.

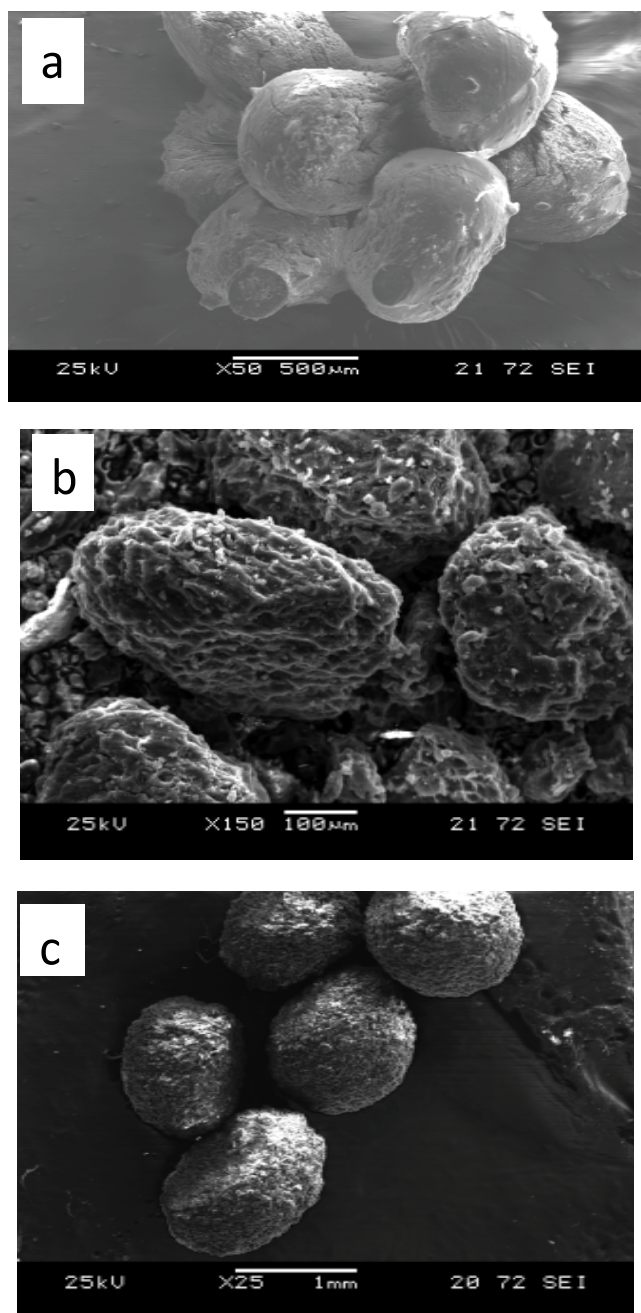


Fig. 2. SEM images of the (a) alginate (A), (b) activated carbon (AC), and (c) A-AC composite beads.

from this plot, the BPA and TCP removal was found to decrease with an increase in initial solution pH from 2 to 10. In this study, the highest BPA and TCP removal was achieved at pH 2, with maximum removal of 97.8%. Similar results have been reported for the adsorption of 2,4-DCP and 2,4,6-TCP by oil palm empty fruit bunch-based activated carbon [22,23], palm pith carbon [24], and Cattail fiber [25]. The pH_{pzc} for A-AC was 4.45 (Fig. 3. inset). At pH below 4.45, the A-AC surface is positively charged, and at $pH < pK_a$ (9.6–10.2) of BPA and $pH < pK_a$ (6.7–6.94) of TCP, the EDCs compounds are in the non-dissociated

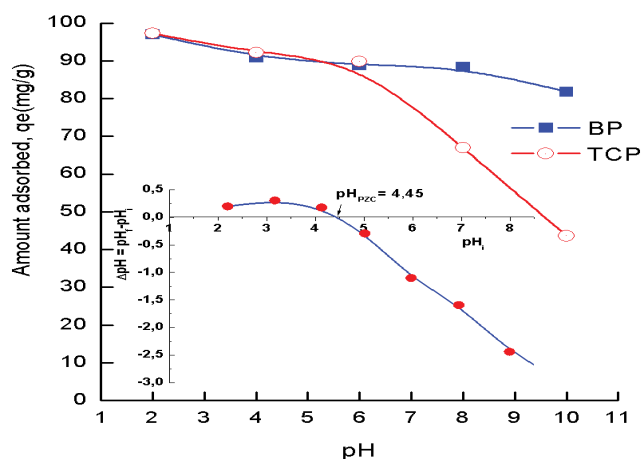


Fig. 3. Effect of initial pH on BPA/TCP removal from solution by A-AC. Inset shows the pH_{pzc} of the A-AC composite beads.

forms. In this case, the dispersion interactions predominate in the adsorption process [26,27]. However, at basic pH ($pH > pK_a$), the BPA and TCP dissociate; forming phenolate anions, while the surface functional groups of A-AC are negatively charged. The electrostatic repulsion between identical charges lowers the adsorption capacities. These charges exist between the negative surface charge and the phenolate anions and between phenolate–phenolate anions in the solutions [28]. On the other hand, there might be a competition between the OH^- ions and the ionic species of BPA or TCP, hence reducing BPA and TCP removal amount. Despite these factors, significant removal was observed at alkaline pH, especially for BPA (83% at pH 10), which indicates that physisorption rather than chemisorption might be involved in the removal process [29].

3.3. Effect of contact time and initial concentration

Contact time is an important parameter to determine the equilibrium time and kinetics of the adsorption process. Fig. 4 shows the effect of contact time on the removal of BPA and TCP onto A-AC for different initial concentrations (15, 40, 75, 160, 260, 320, and 400 mg/L) for TCP and (30, 60, 100, 235, 275, and 335 mg/L) for BPA at 25°C. Similar plots are observed for both adsorbates. All plots have the same general feature: a very fast increase in the adsorbed amount at the beginning for all concentrations, followed by a long period of much slower uptake till equilibrium. This phenomenon could be attributed to the abundant availability of active sites on the adsorbent surface. After occupancy of these sites, the remaining vacant sites were difficult to be filled because of the repulsive forces between the solute molecules on the solid phase and consequently, the adsorption became less efficient [30]. The equilibrium period was dependent on initial TCP/BPA concentrations. At TCP/BPA concentration of 15, 40, 75, 160 mg/L and 30, 60, 100 mg/L, the equilibrium time was achieved at 40 h. More TCP/BPA concentrated solutions (260, 320, and 400 mg/L for TCP, 235, 275, and 335 mg/L for BPA) require more time to reach equilibrium (almost 60 h).

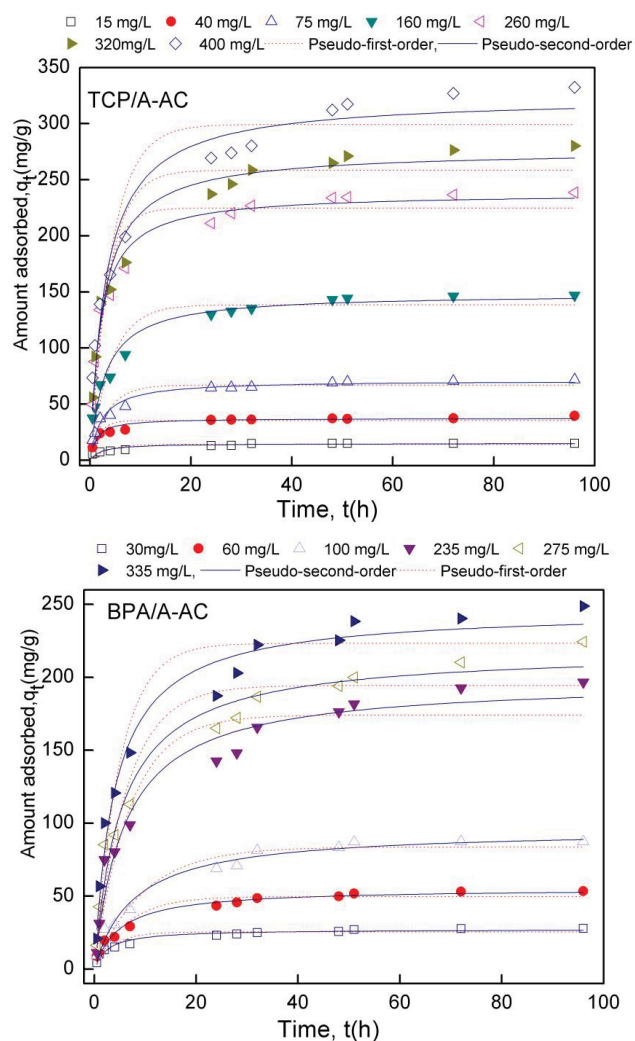


Fig. 4. Effect of contact time on the adsorption of TCP and BPA onto A-AC.

3.4. Kinetics of BPA and TCP adsorption on A-AC

The pseudo-first-order equation [31], pseudo-second-order equation [32], and the intraparticle diffusion model [33], were used to describe the rate of solute uptake at the solid-solution interface.

According to Table 2 and the non-linear fitted plots presented in Fig. 4, it can be seen that the R^2 , RMSE, and AIC values for the pseudo-first-order model did not show a consistent trend and the experimental q_e ($q_{e,exp}$) values did not well agree with the calculated ones ($q_{e,cal}$). This shows that adsorption of the EDCs BPA and TCP onto A-AC does not follow a pseudo-first-order kinetic model. However, the pseudo-second-order model generally provided improved goodness of fit values observed as a reduction of AIC, as well as an increase in the determination coefficient R^2 close to one and with a good agreement between the experimental $q_{e,exp}$ and the calculated $q_{e,cal}$ values. These results indicate that the pseudo-second-order model describes better experimental data. According to previous studies, the pseudo-second-order model assumes that the rate-limiting

step is the chemical binding process involving sharing or exchange of electrons between adsorbent and adsorbate [30]. Several authors reported a successful application of the pseudo-second-order model for the representation of experimental kinetics data of BPA/TCP adsorption on different adsorbents [1,9,10].

In addition, the experimental data were also tested by the intraparticle diffusion model. This model indicates that when the experimental data present linearity and passes through the origin in the graph of q_t vs. $t^{1/2}$, the mechanism of adsorption is controlled by intraparticle diffusion. According to this model [33], the plots of q_t vs. $t^{1/2}$ (Fig. 5.) are non-linear for the whole range of studied concentrations, indicating that intraparticle diffusion is not the only-limiting step, but another process may also be involved in the adsorption process [19]. It was observed that there were three sections in the curves represented by straight lines, indicating the BPA and TCP were transported to macro-, meso- and then slowly diffused into micropores [33]. The values of k_3 were determined from the slopes of the linear plots and presented in Table 3. This table shows the obtained values of k_3 generally increased as the initial BPA or TCP concentration increased, which can be attributed to the greater driving force.

3.5. Adsorption isotherm studies

Adsorption isotherm studies were done to predict the interactions between the adsorbate molecules and the surface of the adsorbent material. In this part, the adsorption isotherms of BPA and TCP onto A-AC were studied in single and binary systems.

3.5.1. Single system

The non-linear form of the Langmuir [34], Freundlich [35], Sips [36], and Redlich–Peterson [37] isotherm models are presented in S.M. From the AIC, R^2 , and RMSE values, it is indicated that the adsorption data are well fitted with Langmuir model for TCP and BPA (Table 4) indicating monolayer molecular adsorption of BPA and TCP on A-AC surface. As shown in Table 4, the predicted maximum adsorption capacity of A-AC at 298 K obtained by the Langmuir model is 419.6 mg/g for BPA and 444.7 mg/g for TCP. The q_{max} values in single compound systems indicated that the active sites of the A-AC are more selective for TCP than BPA [38]. Adsorption intensity parameters ($1/n$) evaluated from the Freundlich model were ranged between 0 and 1 (0.453 for TCP and 0.593 for BPA), confirming the favorable adsorption process. The Redlich–Peterson isotherm was developed to improve the fit between Langmuir and Freundlich equations. If the value of its parameter $g = 1$, then the Langmuir model is better, if $g = 0$, then the Freundlich model is better. In our case, $g = 1.6$, and 1.1 for BPA and TCP, respectively, which indicates that the Langmuir model is more adequate. The Sips isotherm is a combination of Langmuir and Freundlich isotherms. The value of q_m determined by Sips model is 432.6 mg/g for BPA and 479.4 mg/g for TCP, it is slightly higher than that determined by the Langmuir model and the experimental value. From the analysis of all these isotherms, we conclude that the model of

Table 2
Adsorption kinetics of TCP and BPA onto A-AC beads

EDCs		Pseudo-first-order model					Pseudo-second-order model				
BPA C ₀	q _{exp}	q _{cal}	k ₁	RMSE	AIC	R ²	q _{e,cal}	k ₂ 10 ³	RMSE	R ²	AIC
30	28.3	25.5	0.265	2.49	24.876	0.928	27.3	13.7	1.53	0.973	13.191
60	53.3	49.7	0.157	3.95	35.899	0.957	55.4	3.6	2.42	0.984	24.193
100	94.0	86.3	0.093	6.62	45.8855	0.962	99.42	1.2	4.3	0.984	36.634
235	186.4	170.6	0.153	15.60	71.643	0.948	191.95	0.95	10.2	0.978	61.393
275	214.1	192.4	0.163	17.13	73.128	0.949	215.21	0.92	10.6	0.980	62.234
335	247.9	223.4	0.201	19.27	73.964	0.951	246.3	1.0	11.8	0.981	62.236
TCP C ₀	q _{exp}	q _{cal}	k ₁	RMSE	AIC	R ²	q _{e,cal}	k ₂ 10 ³	RMSE	R ²	AIC
15	14.6	14.2	0.29	1.82	17.32	0.760	15.0	31.2	1.28	0.932	8.864
40	40.1	35.5	0.57	3.85	35.285	0.790	37.4	22.1	2.28	0.963	22.78
75	72.5	67.0	0.30	5.93	45.591	0.896	71.2	6.21	3.3	0.980	31.580
160	147.7	138.5	0.24	12.71	63.989	0.897	148.4	2.35	7.97	0.974	52.771
260	239.2	224.8	0.35	17.74	71.979	0.916	238.3	2.14	8.64	0.988	54.710
320	285.6	259.6	0.27	24.7	79.334	0.894	277.8	1.38	14.54	0.976	66.35
400	323.8	297.3	0.23	29.24	84.883	0.881	320.9	1.02	18.28	0.971	73.976

C₀ (mg/L), q_e (mg/g), k₁ (1/h), k₂ (g/mg/h).

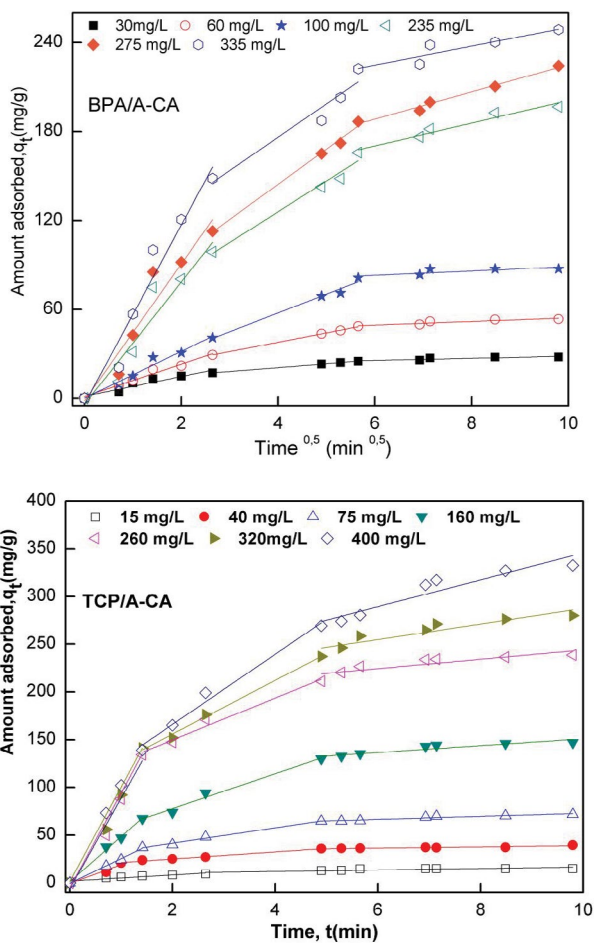


Fig. 5. Intraparticle diffusion model for TCP and BPA adsorption onto A-AC.

Langmuir is the most plausible to describe the isotherm data of BPA and TCP adsorption onto A-AC in single systems.

3.5.2. Binary system

The presence of diverse micropollutants in the solution can simultaneously affect the affinity and the adsorption capacity of the adsorbent. Therefore, the competitive adsorption of emerging compounds in the mixtures of BPA/TCP onto A-AC was investigated. The experiments were performed by fixing either the concentration of BPA at 50 mg/L and varying that of TCP or by fixing the concentration of TCP (50 mg/L) and varying that of BPA. The effect of competitive adsorption of BPA and TCP onto A-AC are shown in Fig. 6. The isotherm data of the binary solution systems were analyzed using the Langmuir (Eq.SM1), Freundlich (Eq.SM2), and extended Langmuir models (Eqs. (11) and (12)).

The extended Langmuir model can be expressed as [39]:

$$q_{e,1} = \frac{q_{m,1} \times K_{L,1} \times C_{e,1}}{1 + K_{L,1}C_{e,1} + K_{L,2}C_{e,2}} \tag{11}$$

$$q_{e,2} = \frac{q_{m,2} \times K_{L,2} \times C_{e,2}}{1 + K_{L,1}C_{e,1} + K_{L,2}C_{e,2}} \tag{12}$$

where $K_{L,1}$, $K_{L,2}$, $q_{m,1}$ and $q_{m,2}$ are the Langmuir isotherm model parameters obtained from Eq. (13) in the single solute system. From Eqs. (11) and (12), we have Eq. (13):

$$\frac{K_{L,2}C_{e,2}}{K_{L,1}C_{e,1}} = \frac{q_{m,1}q_{e,2}}{q_{m,2}q_{e,1}} \tag{13}$$

The linear form of extended Langmuir isotherm in binary system Eq. (11) was obtained [40]:

Table 3
Intraparticle diffusion parameters for the adsorption of TCP and BPA onto A-AC beads

Intraparticle diffusion model				
BPA concentration C_0	k_3	C	RMSE	R^2
30	2.7	7.0	3.74	0.840
60	5.6	9.4	6.31	0.891
100	9.9	10.5	10.12	0.907
235	20.9	25.3	20.83	0.912
275	23.0	32.0	23.31	0.909
335	25.5	45.0	31.46	0.870
TCP Concentration C_0	k_3	C	RMSE	R^2
15	1.4	4.6	2.06	0.823
40	3.2	14.4	6.31	0.721
75	6.7	20.7	10.4	0.808
160	14.3	38.4	19.9	0.840
260	22.0	73.7	38.3	0.770
320	26.8	73.4	38.5	0.831
400	32.2	76.3	37.7	0.881

k_3 (mg/g/h^{1/2}), k_4 (1/h)

$$\frac{C_{e,1}}{q_{e,1}} = \frac{1}{K_{L,1}q_{m,1}} + \frac{C_{e,1}}{q_{m,1}} + \frac{q_{e,2}C_{e,1}}{q_{e,1}q_{m,2}} \quad (14)$$

The affinity of the adsorbent toward the particular components in the binary systems is indicated by the selectivity ratio ($S_{(i,j)}$). Based on the morphology, surface structure, and pore distribution of an adsorbent, selectivity ratio investigates the adsorbent preference toward one solute in the presence of another [42–43], which is defined as:

$$S_{(i,j)} = \frac{Q_{i,b}}{Q_{j,b}} = \frac{Q_{i,s}}{Q_{j,s}} \quad (15)$$

where $Q_{i,b}$ and $Q_{i,s}$ represent the adsorption capacity of component i in the binary and single-component solution. The value of $S_{(i,j)}$ being less than one implies that the adsorbent has more affinity toward component j than the component i [44].

According to Eq. (11), the values of $C_{e,1}/q_{e,1}$ had a linear correlation with $C_{e,1}$ and $q_{e,2}C_{e,1}/q_{e,1}q_{m,2}$ if the adsorption describes the extended Langmuir model. According to Fig. 10 and the high values of R^2 , the adsorption of BPA and TCP from binary solutions was best described by the Langmuir isotherm model, indicating that the adsorbate molecules were adsorbed at well-defined sites and without interactions between those adsorbed on adjacent sites [38]. In addition, the values of q_e^b (binary solution system)/ q_e^s (single solution system) for both BPA (0.6949) and TCP (0.9673) were found to be less than 1.0, suggesting that simultaneous presence of both BPA and TCP molecules reduced the adsorption capacity through competition for binding sites on the A-AC. According to the obtained results (Table 4), the Langmuir model fitted well the binary

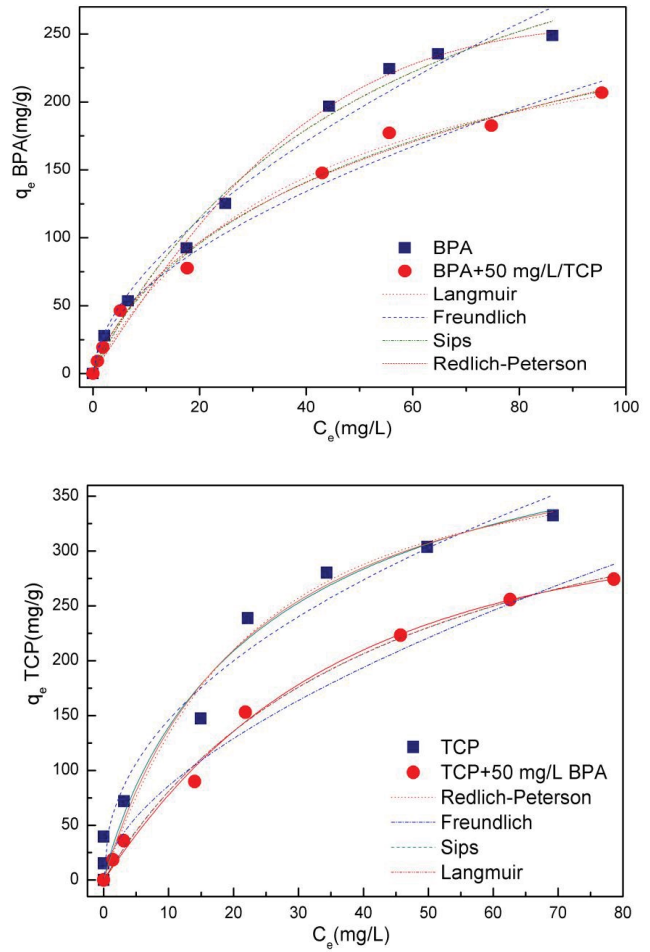


Fig. 6. Adsorption isotherms of BPA and TCP onto A-AC in single and binary systems.

system isotherms data. These results showed that the binary system adsorption onto A-AC is monolayer and homogeneous in nature. Compared to those of the single emerging compound system, the q_{max} values of the two compounds decreased in binary systems. The q_{max} of TCP and BPA decreased from 444.7 to 430.2 mg/g and from 419.6 to 291.5 mg/g, respectively. This means that the adsorption of TCP or BPA onto A-AC was affected by the presence of BPA or TCP, respectively. The results indicate that there is a competition between the EDCs for the adsorption sites on A-AC [36]. The results confirm also that the preferential adsorption by A-AC was given to TCP. This difference in behavior is probably attributed to the values of octanol-water partitioning coefficients ($\log K_{ow}$) of each compound, which results in different hydrophobic interaction densities with A-AC adsorbent. Indeed, TCP is more hydrophobic ($K_{ow} = 3.66$) than BPA ($K_{ow} = 3.32$). This difference determines the extent of the adsorption affinity, resulting in the preferential adsorption of TCP. Similar results have been reported in previous works [2]. This is corroborated by the estimated selectivity ratio, $S_{(i,j)}$ value of TCP (1.05), which is greater than unity, whereas, its value for BPA (0.90) is less than one. The results confirmed that the A-AC adsorbent

has more affinity toward TCP than BPA. Similar antagonistic analogous trends could be noticed also in the binary dyes solution of remazol brilliant blue (RBB) and disperse orange (DO) [45], methylene blue (MB), and methyl orange (MO) [46], and methyl orange (MO) and phenol [42].

3.6. Comparison of adsorption of BPA and TCP on various adsorbents

Table 5 lists the maximum monolayer adsorption capacities for TCP and BPA on various adsorbents. The high adsorption capacity of A-AC found in this study reveals that this composite is a promising adsorbent for TCP and BPA removal.

Table 4
Langmuir, Freundlich, Sips, Redlich–Peterson, and extended Langmuir isotherm parameters for the adsorption of TCP and BPA onto A-CA beads in single and binary systems

Parameters	BPA	BPA + 50 mg/L TCP	TCP	TCP + 50 mg/L BPA
Langmuir				
q_{max}	419.6	291.5	444.7	430.2
K_L	0.019	0.025	0.045	0.023
R^2	0.989	0.989	0.972	0.994
RMSE	9.76	8.26	22.30	8.18
AIC	49.55	46.54	64.43	43.33
Freundlich				
K_F	19.55	18.0	51.4	40
$1/n$	0.593	0.55	0.453	0.4
R^2	0.982	0.988	0.963	0.890
RMSE	13.120	9.450	25.620	13.160
AIC	54.87	48.97	66.91	50.93
Sips				
q_{max}	432.6	398.0	479.4	437.5
K_S	0.019	0.029	0.05	0.023
m	0.976	0.792	0.908	0.985
R^2	0.987	0.991	0.967	0.993
RMSE	10.53	7.740	23.980	8.957
AIC	56.73	51.19	71.54	52.65
Redlich–Peterson				
A_{RP}	5.99	11.69	17.19	8.74
B_{RP}	0.0006	0.1640	0.0220	0.0078
g	1.66	0.72	1.1	1.2
R^2	0.990	0.990	0.966	0.993
RMSE	9.290	8.22	24.030	8.685
AIC	54.47	52.28	71.57	52.16
Extended Langmuir				
$q_{m,i}$		257.1		392.2
$K_{L,i}$		0.036		0.029
R^2		0.965		0.956

3.7. Thermodynamics of adsorption

The thermodynamic parameters were estimated to evaluate the feasibility and nature of the adsorption process. Gibbs free energy (ΔG° , kJ/mol), enthalpy (ΔH° , kJ/mol), and entropy (ΔS° , kJ/mol) changes were calculated at various temperatures (288, 298, 308, and 318 K) and were estimated using the following equations [8]:

$$\Delta G = -RT \ln K \quad (16)$$

$$\text{Log} \left(\frac{1,000 \times q_e}{C_e} \right) = \frac{\Delta S^\circ}{2.303R} - \frac{\Delta H^\circ}{2.303RT} \quad (17)$$

where q_e is the adsorbed amount of BPA or TCP per unit of mass of A-AC (mg/g), C_e is the equilibrium concentration of TCP or BPA (mg/L), R is the universal gas constant (8.314 J/mol K), and T is the temperature in Kelvin (K).

By investigating the plot of $\text{Log}(1,000 \times q_e / C_e)$ vs. $1/T$ ($R^2 = 0.97$ and 0.92 for BPA and TCP, respectively) (Fig. 7), the intercept and the slope values were used to calculate ΔH° and ΔS° , respectively. The thermodynamic parameters are listed in Table 6. The values of ΔG° are negative, indicating the feasibility of the process and suggesting that the adsorption of BPA and TCP onto A-AC is a spontaneous and physical process. The positive values of ΔH° (24.2 and 26.0 kJ/mol for BPA and TCP, respectively) indicate that the adsorption process is endothermic in nature. The positive values of ΔS° suggest that the degree of freedom increases at the solid–liquid interface during the adsorption of TCP and BPA.

3.8. Adsorbent regeneration

The regeneration step is an important process used to restore the adsorption capacity. The viability of regenerating the exhausted A-AC saturated with both TCP and BPA was evaluated using the ethanol desorption technique. The results of the regeneration studies are graphically

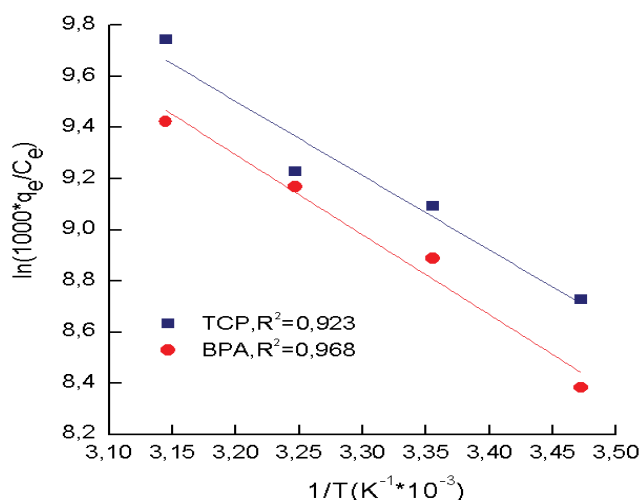


Fig. 7. Effect of temperature on the adsorption of BPA and TCP onto A-AC.

Table 5
Comparison of the adsorption capacity of A-AC with various adsorbents for BPA/TCP removal

EDCs	Adsorbents	C_0 (mg/L)	Isotherm model	Kinetic model	q_m (mg/g)	Reference
BPA	Calcium alginate/activated carbon (A-AC)	30–300	L	Ps2	419.6	This study
	β -Cyclodextrin capped graphene-magnetite	10–200	L	Ps2	59.6	[39]
	Activated carbon prepared from potato peels	0–300	L	Ps2	454.62	[40]
	Graphene	10–500	L	Ps2	94.06	[41]
	Montmorillonite Modified with DDDMA	5–500	L	Ps2	256.41	[42]
TCP	Calcium alginate/activated carbon (A-AC)	15–400	L	Ps2	444.7	This study
	Bentonite	10–250	L	Ps2	200.6	[43]
	MgAl-SDBS organo-layered double hydroxides	10–250	L	Ps2	240.5	[10]
	Organo-montmorillonite	25–300	L	Ps2	368	[44]
	Organophilic-bentonite	10–100	L	Ps2	72.14	[9]

L: Langmuir, Ps2: Pseudo-second order

Table 6
Thermodynamic parameters for the adsorption of TCP and BPA onto A-AC beads

EDCs	T (K)	ΔG° (kJ/mol)	ΔH° (kJ/mol)	ΔS° (J/mol K)
TCP	288	–20.86	24.18	156.40
	298	–22.42		
	308	–23.99		
	318	–25.55		
BPA	288	–20.21	26.01	160.49
	298	–21.82		
	308	–23.42		
	318	–25.03		

presented in Fig. 8. This figure shows BPA and TCP adsorption removal (%) for six cycles of successive adsorption/desorption. It can be observed that the amount of desorbed BPA or TCP was quite high and that the total adsorption capacities are slightly decreased (11% and 7% for BPA and TCP, respectively) after the sixth regeneration. This small drop in adsorption capacities could be ascribed to the fact that the regeneration process might result in a decrease of binding sites [37,39]. Furthermore, regeneration experiments confirm the good stability of A-AC after multicycle tests.

4. Conclusion

In this study, the removal of BPA and TCP from aqueous solution in single and binary solution systems, using the eco-friendly composite adsorbent material (A-AC) was investigated. The adsorption of BPA and/or TCP from aqueous solutions was found to be feasible, especially in an acidic medium. In fact, it decreased as the pH increased due to the simultaneous change in A-AC surface charges and partial solute ionization. The pseudo-second-order model fitted well the experimental kinetics data. The removal of BPA and TCP from aqueous solution by A-AC increased with increasing temperature, indicating that an endothermic

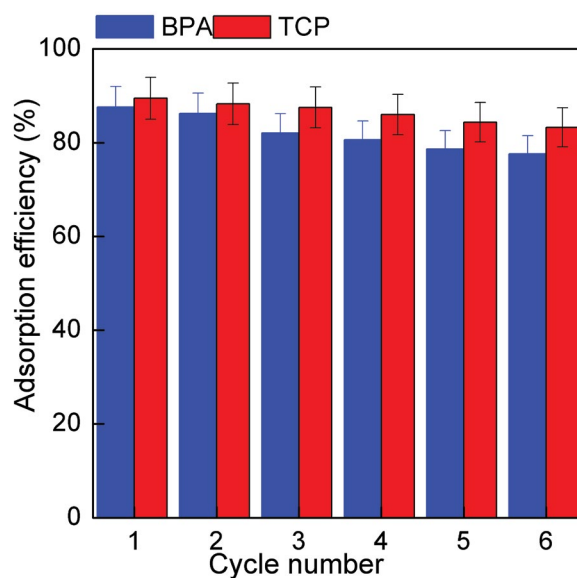


Fig. 8. Adsorption/desorption cycles of BPA and TCP onto A-AC.

process occurred. The equilibrium adsorption data were well-fitted to the Langmuir model and the monolayer saturation capacities were found to be 419.3 and 444.7 mg/g for BPA and TCP, respectively. The obtained data from the adsorption–desorption experiments illustrate the efficient and stabilized performance of A-AC during repeated cycles. The present study concludes that the A-AC composite significantly removes BPA and TCP compounds from aqueous solutions and shows excellent regeneration capacity. This composite may be used as an efficient and economic adsorbent for the removal of BPA and TCP from water in single and binary systems.

Acknowledgments

The authors thank the Laboratory of Chemical Engineering (LGPC) and the University of Setif, Algeria for financial support.

References

- [1] A. Bhatnagar, I. Anastopoulos, Adsorptive removal of bisphenol A (BPA) from aqueous solution: a review, *Chemosphere*, 168 (2017) 885–902.
- [2] N. Djebri, M. Boutahala, N.-E. Chelali, N. Boukhalifa, L. Zerroual, Adsorption of bisphenol A and 2,4,5-trichlorophenol onto organo-acid-activated bentonite from aqueous solutions in single and binary systems, *Desal. Water Treat.*, 66 (2017) 383–393.
- [3] N. Djebri, N. Boukhalifa, M. Boutahala, D. Hauchard, N.-E. Chelali, A. Kahoul, Calcium alginate-organobentonite-activated carbon composite beads as a highly effective adsorbent for bisphenol A and 2,4,5-trichlorophenol: kinetics and equilibrium studies, *Desal. Water Treat.*, 83 (2017) 294–305.
- [4] M. Zielinska, K. Bułkowska, A. Cydzik-Kwiatkowska, K. Bernat, I. Wojnowska-Baryła, Removal of bisphenol A (BPA) from biologically treated wastewater by microfiltration and nanofiltration, *Int. J. Environ. Sci. Technol.*, 13 (2016) 2239–2248.
- [5] S. Yüksel, N. Kabay, M. Yüksel, Removal of bisphenol A (BPA) from water by various nanofiltration (NF) and reverse osmosis (RO) membranes, *J. Hazard. Mater.*, 263 (2013) 307–310.
- [6] J. Sharma, I. Mishra, V. Kumar, Degradation and mineralization of Bisphenol A (BPA) in aqueous solution using advanced oxidation processes: UV/H₂O₂ and oxidation systems, *J. Environ. Manage.*, 156 (2015) 266–275.
- [7] M. Umar, F. Roddick, L. Fan, H.A. Aziz, Application of ozone for the removal of bisphenol A from water and wastewater: a review, *Chemosphere*, 90 (2013) 2197–2207.
- [8] N. Djebri, M. Boutahala, N.-E. Chelali, N. Boukhalifa, L. Zerroual, Enhanced removal of cationic dye by calcium alginate/organobentonite beads: modeling, kinetics, equilibria, thermodynamic and reusability studies, *Int. J. Biol. Macromol.*, 92 (2016) 1277–1287.
- [9] H.Z. Boudiaf, M. Boutahala, Equilibrium and kinetics studies of 2,4,5-trichlorophenol adsorption onto organophilic-bentonite, *Desal. Water Treat.*, 24 (2010) 47–54.
- [10] H. Zaghouane-Boudiaf, M. Boutahala, C. Tiar, L. Arab, F. Garin, Treatment of 2,4,5-trichlorophenol by MgAl-SDBS organo-layered double hydroxides: kinetic and equilibrium studies, *Chem. Eng. J.*, 173 (2011) 36–41.
- [11] H.Z. Boudiaf, M. Boutahala, Kinetic analysis of 2,4,5-trichlorophenol adsorption onto acid-activated montmorillonite from aqueous solution, *Int. J. Miner. Process.*, 100 (2011) 72–78.
- [12] H.Z. Boudiaf, M. Boutahala, Preparation and characterization of organo-montmorillonites. Application in adsorption of the 2,4,5-trichlorophenol from aqueous solution, *Adv. Powder Technol.*, 22 (2011) 735–740.
- [13] J.R. Koduru, L.P. Lingamdinne, J. Singh, K.-H. Choo, Effective removal of bisphenol A (BPA) from water using a goethite/activated carbon composite, *Process Saf. Environ. Prot.*, 103 (2016) 87–96.
- [14] K.L. Chang, J.F. Hsieh, B.M. Ou, M.H. Chang, W.Y. Hsieh, J.H. Lin, P.J. Huang, K.F. Wong, S.T. Chen, Adsorption studies on the removal of an endocrine-disrupting compound (bisphenol A) using activated carbon from rice straw agricultural waste, *Sep. Sci. Technol.*, 47 (2012) 1514–1521.
- [15] N. Boukhalifa, M. Boutahala, N. Djebri, A. Idris, Maghemite/alginate/functionalized multiwalled carbon nanotubes beads for methylene blue removal: adsorption and desorption studies, *J. Mol. Liq.*, 275 (2019) 431–440.
- [16] N. Boukhalifa, M. Boutahala, N. Djebri, A. Idris, Kinetics, thermodynamics, equilibrium isotherms, and reusability studies of cationic dye adsorption by magnetic alginate/oxidized multiwalled carbon nanotubes composites, *Int. J. Biol. Macromol.*, 123 (2019) 539–548.
- [17] A. Benhouria, M. Azharul Islam, H.Z. Boudiaf, M. Boutahala, B.H. Hameed, calcium alginate-bentonite-activated carbon composite beads as highly effective adsorbent for methylene blue, *Chem. Eng. J.*, 270 (2015) 621–630.
- [18] O. Duman, S. Tunc, T.G. Polat, B.K. Bozoglan, Synthetic of magnetic oxidized multiwalled carbon nanotube-K-carrageenan-Fe₃O₄ nanocomposite adsorbent and its application in cationic methylene blue dye adsorption, *Carbohydr. Polym.*, 147 (2016) 79–88.
- [19] H. Shao, Y. Li, L. Zheng, T. Chen, J. Liu, Removal of methylene blue by chemically modified defatted brown algae *Laminaria japonica*, *J. Taiwan Inst. Chem. Eng.*, 80 (2017) 525–532.
- [20] N. Belhouchat, H. Zaghouane-Boudiaf, C. Viseras, Removal of anionic and cationic dyes from aqueous solution with activated organo-bentonite/sodium alginate encapsulated beads, *Appl. Clay Sci.*, 135 (2017) 9–15.
- [21] M. Lezehari, J.P. Basly, M. Baudu, O. Bouras, Alginate encapsulated pillared clays: removal of a neutral/anionic biocide (pentachlorophenol) and a cationic dye (safranin) from aqueous solutions, *Colloids Surf., A*, 366 (2010) 88–94.
- [22] I.A.W. Tan, A.L. Ahmad, B.H. Hameed, Adsorption isotherms, kinetics, thermodynamics and desorption studies of 2,4,6-trichlorophenol on oil palm empty fruit bunch-based activated carbon, *J. Hazard. Mater.*, 164 (2009) 473–482.
- [23] F.W. Shaarani, B.H. Hameed, Batch adsorption of 2,4-dichlorophenol onto activated carbon derived from agricultural waste, *Desalination*, 255 (2010) 159–164.
- [24] M. Sathishkumar, A.R. Binupriya, D. Kavitha, S.E. Yun, Kinetic and isothermal studies on liquid-phase adsorption of 2,4-dichlorophenol by palm pith carbon, *Bioresour. Technol.*, 98 (2007) 866–873.
- [25] L. Ren, J. Zhang, Ye Li, C. Zhang, Preparation and evaluation of cattail fiber-based activated carbon for 2,4-dichlorophenol and 2,4,6-trichlorophenol removal, *Chem. Eng. J.*, 168 (2011) 553–561.
- [26] K. Laszlo, A. Szucs, Surface characterization of poly-ethyleneterephthalate (PET) based activated carbon and the effect of pH on its adsorption capacity from aqueous phenol and 2,3,4-trichlorophenol solutions, *Carbon*, 39 (2001) 1945–1953.
- [27] K. Laszlo, P. Podkoscielny, A. Dabrowski, Heterogeneity of polymer-based active carbons in adsorption of aqueous solutions of phenol and 2,3,4-trichlorophenol, *Langmuir*, 19 (2003) 5287–5294.
- [28] B.H. Hameed, I.A.W. Tan, A.L. Ahmad, Adsorption isotherm, kinetic modeling and mechanism of 2,4,6-trichlorophenol on coconut husk-based activated carbon, *Chem. Eng. J.*, 144 (2008) 235–244.
- [29] Z.N. Garba, A.A. Rahim, Optimization of activated carbon preparation conditions from *Prosopis africana* seed hulls for the removal of 2,4,6-trichlorophenol from aqueous solution, *Desal. Water Treat.*, 56 (2015) 2879–2889.
- [30] S. Sahnoun, M. Boutahala, Adsorption removal of tartrazine by chitosan/polyaniline composite: kinetics and equilibrium studies, *Int. J. Biol. Macromol.*, 114 (2018) 1345–1353.
- [31] S. LARGERGREN, On the theory of so-called adsorption of solutes, *Kungl. Svenska Vetenskapsakademiens Handlingar*, 24 (1898) 1–39.
- [32] Y.S. Ho, G. McKay, Pseudo-second-order model for adsorption processes, *Process Biochem.*, 34 (1999) 451–465.
- [33] W.J.J. Weber, J.C. Morris, Kinetics of adsorption on carbon from solution, *J. Sanitary Eng. Div.*, 89 (1963) 31–59.
- [34] I. Langmuir, The constitution and fundamental properties of solids and liquids, *J. Am. Chem. Soc.*, 38 (1916) 2221–2295.
- [35] H.M.F. Freundlich, Über die adsorption in loesungen, *Z. Phys. Chem.*, 57 (1906) 385–470.
- [36] R. Ghemit, A. Makhloufi, N. Djebri, A. Fllissa, L. Zerroual, Adsorptive removal of diclofenac and ibuprofen from aqueous solution by organobentonites: study in single and binary systems, *Groundwater Sustainable Dev.*, 8 (2019) 520–529.
- [37] X. Zheng, J. Dai, J. Pan, Synthesis of b-cyclodextrin/mesoporous attapulgite composites and their novel application in adsorption of 2,4,6-trichlorophenol and 2,4,5-trichlorophenol, *Desal. Water Treat.*, 57 (2016) 14241–14250.
- [38] A.A. Oladipo, E.O. Ahaka, M. Gazi, High adsorptive potential of calcined magnetic biochar derived from banana peels for Cu²⁺, Hg²⁺ and Zn²⁺ ions removal in single and ternary systems, *Environ. Sci. Pollut. Res.*, 26 (2019) 31887–31899.
- [39] Y. Zhou, P. Lu, J. Lu, Application of natural biosorbent and modified peat for bisphenol A removal from aqueous solutions, *Carbohydr. Polym.*, 88 (2012) 502–508.

- [40] H. El Fargani, R. Lakhmiri, H. El Farissi, A. Albourine, M. Safi, O. Cherkaoui, Removal of anionic dyes by silica-chitosan composite in single and binary systems: valorization of shrimp co-product "*Crangon crangon*" and "*Pandalus borealis*", J. Mater. Environ. Sci., 8 (2017) 724–739.
- [41] A.T. Sdiri, T. Higashi, F. Jamoussi, Adsorption of copper and zinc onto natural clay in single and binary systems, Int. J. Environ. Sci. Technol., 11 (2014) 1081–1092.
- [42] R. Istratie, M. Stoia, C. Pa, Single and simultaneous adsorption of methyl orange and phenol onto magnetic iron oxide/carbon nanocomposites, Arabian J. Chem., 12 (2019) 3704–3722.
- [43] L. Zhang, J. Wei, X. Zhao, F. Li, F. Jiang, M. Zhang, X. Cheng, Competitive adsorption of strontium and cobalt onto tin antimonite, Chem. Eng. J., 285 (2016) 679–689.
- [44] C.R. Girish, Simultaneous adsorption of pollutants onto the adsorbent: review of interaction mechanism between the pollutants and the adsorbent, Int. J. Eng. Technol., 7 (2018) 3613–3622.
- [45] R.G. Mavinkattimath, V.S. Kodialbail, Simultaneous adsorption of remazol brilliant blue and disperse orange dyes on red mud and isotherms for the mixed dye system, Environ. Sci. Pollut. Res., 24 (2017) 18912–18925.
- [46] M. Ahmaruzzaman, R.A. Reza, Decontamination of cationic and anionic dyes in single and binary mode from aqueous phase by mesoporous pulp waste, Environ. Prog. Sustainable Energy, 34 (2015) 724–735.